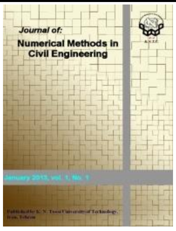

Numerical Methods in Civil Engineering

Study on the Structural Behaviour of the Topside Modules of FPSO under the Forces Exerted on the Ship Hull

***Mahdi Saleh*[*]*, Rouhollah Amirabadi*[**]*, Abbas Kheiri*[***]**

ARTICLE INFO

Article history:
Received:
April 2020.
Revised:
May 2020.
Accepted:
June 2020.

Keywords:
Floating Production Storage and Offloading
FPSO
Topside Module
Quasi-static analysis

Abstract:

The extraction of oil and gas from deep water is one of the most important challenges of the oil and gas industry today. FPSO is one of the leading platforms for deep waters. This study discussed the performance of FPSO deck modules under loads exerted on the hull of the ship. Modeling of the studied module was executed by SACS software and the effect of support using neoprene in the function of the module's members was studied. The members of this module are divided into two general areas: the first area includes fulcrum members under the main deck of module and the second area includes installed members on the main deck and equipment of the module which is investigated in three directions; longitudinal, transverse and vertical. After analysis, it was confirmed that in the module which uses neoprene, the connected members to the neoprene have a significant decrease in relative stress, whereas, the transverse members exhibited increased relative stress. On the other hand, the vertical and longitudinal members displayed insignificant changes.

1. Introduction

Considering the importance of oil and gas extraction, research in this area is vital. Many oil and gas resources are in deep water that cannot be extracted using conventional structures. One of the best solutions is using floating structures in deep water. This paper examines the FPSO platform as one of the most popular deep-water platforms.

In 1996, Lapidier et al examined floating platforms. They stated that there is extensive experience in the field of oil and gas extraction in the design and construction of fixed platforms; therefore, they examined platforms, floating vessels and the impact of waves on them [1]. Then Orbek et al in 2000 reviewed and presented a standard separate from the rules of the existing names for the design of offshore structures [2]. Welford et al in 2001 reviewed the design of structures on the decks of the FPSO platforms and other marine structures. In this type of acceptable level of risk, design was adopted based on a laboratory model [3].

**PhD student, Faculty of Civil Engineering, University of Qom, Qom, Iran.*
***Corresponding Author: Assistance professor, Faculty of Civil Engineering, University of Qom, Qom, Iran, Email: r.amirabadi@qom.ac.ir.*
****MSc, Avantgarde Petro Energy Kish Company*

Francois et al are reviewing the FPSO design rules and regulations. In 2002, they stated that this kind of platform, despite the appearance of the ship, was due to differences in their functions, and should be included in the regulations for ship design, which would be used in design [4]. In 2002, Han et al explored a specific type of FPSO platform for the extraction and storage of liquid gas. This type of platform is called FSRU. They stated that due to the increasing demand for natural gas in many countries, extraction of these resources from deep water is extremely important. They considered the FSRU to be a scientific and economical solution to this challenge [5]. Then in 2002, Kirkle et al examined the structure of the junction of the ship-mounted modules on the deck and focused on this issue. They recognized the basic concepts of deck structures and examined the results of making changes to each of the designs [6]. While the use of FPSO was developing, considerable attention was paid to increasing the speed of construction and installation. In 2003 Thomas et al provided a solution for FPSO Module Integration [7] and Wang et al researched a condition where the interest of the design and use of FPSO platforms was increasing but there was a shortage of suitable data available to design these platforms.

Therefore, in 2003, they focused on providing and reviewing data on commercial tankers that could be used to design FPSO platforms [8]. Back in 2003, Thomas et al presented a method for installing modules based on the FPSO platform decks. The proposed method has led to a reduction in the cost of constructing and installing equipment on the deck of these platforms [9]. Subsequently, in 2003, Hevigmans studied the hydrodynamics of FPSO platforms fixed in deep waters subjected to regular waves using numerical methods [10]. In 2005, Chakrabartti, in chapter Seven and ten of Handbook of Marine Structures Engineering, explored the design of offshore structures as well as survey equipment on the decks of these platforms, and eventually provided useful information in this area [11]. Bachner et al studied the effects of extreme waves created in deep waters on floating structures in these waters. In 2007, they focused on a numerical approach to investigate the response of the structure to the incoming waves [12]. Afterwards, in 2008, Mouland, in Section 9 of the Marine Engineering Reference Book, addressed issues related to the design, construction and operation of ships, which will be used in the routine study of the subject under study in this research [13]. In the following, Henricksen et al in 2008 carefully examined the structures on the deck of the FPSO platforms under the influence of loads resulting from the deformation of the main beams of the body of the ship, the pressure from existing tankers and the inertial forces of the existing structures on the deck [14]. In 2010, Metzgar investigated and evaluated the risk of developing FPSO platforms for environmental conditions and water depths [15]. Then, Chen et al explored the principles of design and interactions between the modules on the platform deck and provided them with suggestions and solutions in 2011 [16]. In the following, Wagner et al, in 2012, explored the interaction between the structures on the deck and body of the ship. They selected PETROBARS P-53 platform as an option study [17]. In 2013, they explored the loads on ships and offshore structures and evaluated the response of structures due to different loads [18]. After that, Zhong Su et al examined the FPSO for use in deep waters. In 2014, they explored case studies on deck, body, floating systems, anchorage, raiser, and design concepts in the South China Sea [19]. In recent years, special attention has been paid to experimental and nonlinear models. Razieh Zanganeh et al focused on the stability of FPSO under environmental load [20] and J.Sanchez evaluated the dynamic behavior of a FPSO-turret system in an experimental model [22].

The regulations of this field are briefly presented herein: In 2007, the DNV-RP-C101 regulations reviewed the thickness of the body of the ship and Incoming loads to them [23]. Then in 2012, following the revisions to past regulations, the new edition of the DNV-OS-C102 fully addressed the design criteria, Incoming loads, combinations of loads, fatigue phenomena, etc. [24]. The ABS regulations were published in 2014 under the guise of dynamic load guidance on FPSO platforms. This collection deals in detail with the problem of dynamic loads. This version of the regulations modifies the previous version of this collection published in 2010 [25]. Due to the importance of the impact of environmental forces in the design of marine structures, this issue has received much attention today. In this regard, Dezvareh intends to examine the effect of wind turbulence on the aero-hydrodynamic behaviour of offshore wind turbines with a monopile platform [27].

2. Introducing the studied module

The field development shall comprise a three-wells drilling campaign which is expected to last for a period of 75 days, with well heads located on the four–slot unmanned Well Head Platform (WHP) designed for jack-up drilling in cantilever mode making simultaneous drilling and production operations possible. The WHP will be connected to a spread moored FPSO vessel located to the NW, approximately 350 meters away from Platform Centre. The FPSO, orientated in a SE direction will be capable of storing and offloading the produced crude oil.

The FPSO will be moored via a conventional 8-point catenary spread mooring system to allow a safe marine access radius during tandem moored export tanker offloading operations. Shuttle tanker tandem mooring and offloading hoses are designed to be safely released in the event of extreme weather or over-tension.

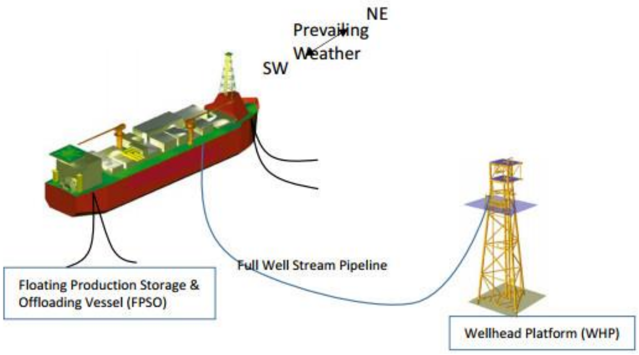

Fig. 1: Facilities of Oil Field

In this study, the CSU module of this platform is discussed and analyzed. This module is on the right side of the ship between the FR148 and FR156 rows, and the L8 and L17. In the main model, this module has four supports with the following features:

- 6.0 m span, between FR148 and FR156 rows
- 6.75 m span, between L8 and L17 rows.
- The module includes three deck levels as detailed below:
- Lower Deck (EL Z = + 21.848 m) supports the following equipment:

- LP Separator
- Flare Scrubber
- HP Separator
- HP Scrubber
- Inlet Heater
- Hydro cyclone
- Chemical Tank

- Mezzanine Deck (EL Z = + 24.848 m) supports Degasser.
- Top Deck (EL Z = + 28.123 m) supports the Expander Pipe.

2-1. Axis System

Global axis system:

- X axis = horizontal and parallel to the Unit longitudinal axis, positive from AFT to FORWARD
- Y axis = horizontal and perpendicular to X axis, positive from hull centerline to PORTSIDE
- Z axis = vertical and positive upwards

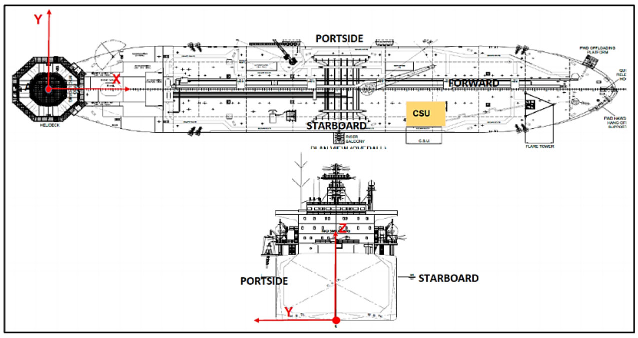

Fig. 2: Axis System and Location of CSU Module

The origin of the axes corresponds to:

- X = 0 at AFT PERPENDICULAR (A.P)
- Y = 0 at the center line of the hull
- Z = 0 at KEEL

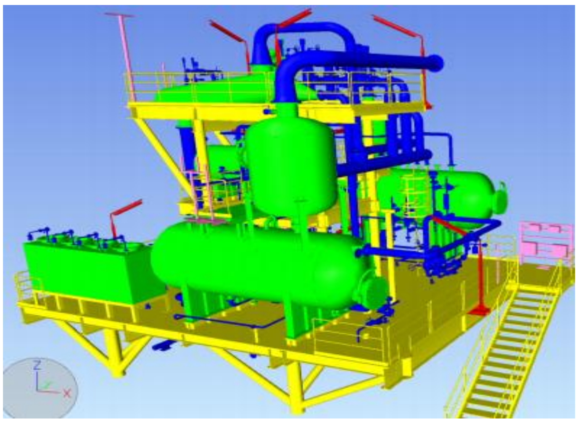

Fig. 3: 3D Model of CSU Module

2-2. Module Local Axis System

The module local coordinate system is originated at starboard-aft corner of the module. The positive x-axis is directed along FPSO longitudinal direction, positive y-axis towards port and positive z-axis upwards from T.O.S. Lower Deck EL (+) 21542 mm.

3. Modeling

3.1- Design Inputs

3.1.1- Design Wind Speed

In table 1 are the referenced wind speed at 10 m above sea level for various averaging periods.

Table 1. Wind Speed for Various Averaging Periods (m/s)

Return Period	1-year	10-year	50-year	100-year
1 hr.	16.0	20.0	22.0	24.0
10 min	18.6	23.2	25.5	27.8
1 min	22.1	27.6	30.4	33.1
3 sec	26.7	33.4	36.7	40.1

The mean wind speed for averaging times shorter than 1h and other elevation may be expressed by the following equation from API RP 2A-WSD [26].

3.1.2 Wind Action

Mean wind actions on the structure may be estimated by calculating the mean wind actions on all exposed components of the structure and summing the contributions from each component.

Mean wind actions on individual components may be calculated using the following equation [26]:

$$F_w = \frac{1}{2}\rho_s U^2 C_s A C_R \qquad (1)$$

Where:

Fw = is the wind action on the object

ρ_s = is mass density of air

U = is the wind speed at height z ASL

C_S = is the shape coefficient

A = is the area of the object

C_R = is the shielding coefficient

3.1.3. Accelerations Values

The hull motion and accelerations for 1 year, 10 years and 50 years return period are provided in terms of linear accelerations at the gravity center of the CSU module and is summarized in table 2. In floating structures, in order to calculate the acceleration caused by the impact of waves, motion analysis is performed first. In the motion analysis report, there is general location table that determines the position of each module on the deck. In the other table the maximum acceleration values for each location are presented. In Table 2, the acceleration values are presented for our studied module location.

Table 2. Acceleration Values for Full Load Condition

Condition	Acceleration Value (g)		
	Ax	Ay	Az
1 Year Transit	0.080	0.078	0.130
10 Years Operating	0.096	0.101	0.166
50 Years Extreme	0.101	0.113	0.179

3.1.4. Deflection Calculation

The maximum deflection of the vessel during Sagging and Hogging condition shall not exceed 1/500 LBP. This would be the worst condition that has been considered in calculating deflection at the stool positions on deck.

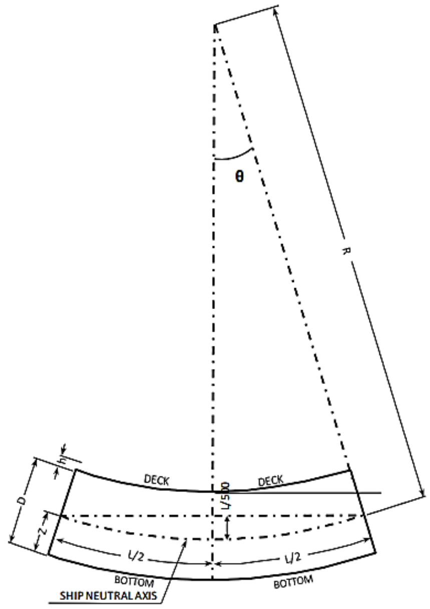

Fig. 4: Illustration of Vessel Deflection in Sagging Condition

In the illustration in Figure 4, the vessel's deflection shape is assumed to be an arc of radius, R, passing through the neutral axis. As the vessel is sagging, the deck of the vessel is in compression and the bottom is in tension. The neutral axis remains the same, i.e., no compression or tension. Similarly, the hogging condition would mirror as illustrated in Figure 4.Vertical and Longitudinal Deflection can cause a force in our module, so, they should be calculated in a location of our studied module.

Table 3. Hull Deflection

X position (m) from Vessel Aft	Q (rad)	SAGGING dx (mm)	SAGGING dz (mm)	HOGGING dx (mm)	HOGGING dz (mm)
112	-0.0024	-22.9	-312.6	22.9	312.6
118	-0.0030	-28.2	-296.4	28.2	296.4

3.1.5. Analysais Method

Linear elastic structural models will be used to determine response for the structure throughout the design conditions. Space frame structures consisting of slender components will be analysed using a 3-D frame analysis to calculate internal component forces and moments. The effect of joint eccentricity and flexibility, where significant, should be accounted for.

3.1.6. Allowable Stresses

The structural steel strength check shall be done using the Working Stress Design (WSD) method. This method is the stress to which material may be safely subjected in the course of ordinary use. The following table summarizes allowable stress factors used for the structural design for all respective conditions.

Table 4. Allowable Stresses for Various Design Conditions

Design Conditions	***Environmental conditions***	***Increased factor on basic allowable stresses***
In-place Operating	10 - year	1.00
In-place Extreme	50 - year	1.33

3.1.7. Boundary Conditions at Interfaces Module and Hull

The module supports are located in special places called the Stools that are mounted on the deck. In this study, a comparison was made between neoprene and fixed support joints. Used Connections in modelling are shown in Figure 5.

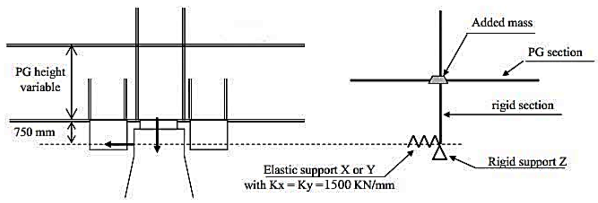

(a)

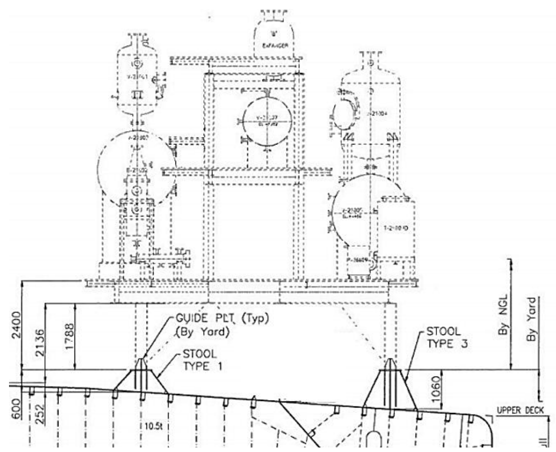

(b)

Fig. 5: Schematic View of CSU Stool and how to connect the module to deck stools using neoprene.

3.1.8. LOADING

3.1.8.1. Summary of Basic Load Cases

The Basic Load Cases considered in the analyses are described in table 5.

3.1.8.2. Load Combinations

In load combinations, four main directions and four diagonal directions are used in accordance with Fig. 6. The acceleration of the diagonal directions is 0.7 times the acceleration of the original direction.

Table 5. Description of Basic Load Cases

Loading Type	Description
Structure	Self-Weight of Model
	Secondary Un-Modeled weight
	Tertiary Un-Modeled weight
Equipment	Equipment – Dry
	Equipment – Content
Piping	Piping – Dry
	Piping – Content
& Electrical Instrument	Electricity & Instrument bulk
Live Loads	Live Load for operating Condition
Wind Loads	Operating wind +X
	Operating wind +Y
	Operating wind –X
	Operating wind –Y
Hull Deflection	Hull Deflection – Sagging
	Hull Deflection - Hogging

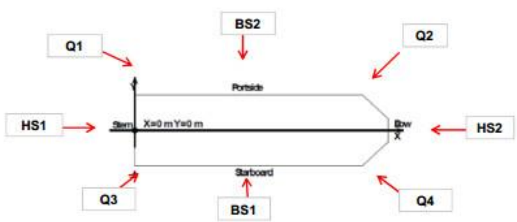

Fig. 6: Load Combinations in 8 directions

3.2. SACS Modelling

In this section, the modelling of the module is studied, and main results are drawn. To check the performance of the studied module when using neoprene, and comparing it with simple support, two models were made. Initially, the main module which has four supports was modelled according to the loading, and then another module under similar loading conditions, was also modelled separately with four supports equipped with Neoprene. In the end, the output of both models are compared with each other and their review charts are presented. It should be noted that modelling has been executed in SACS version 5.7.

3.2.1. First Model

This model has four fixed supports. All assumptions of acceleration, wind speed, weight, etc. are similar to the ones discussed above. Figure 7 represents the overall design and model supports respectively.

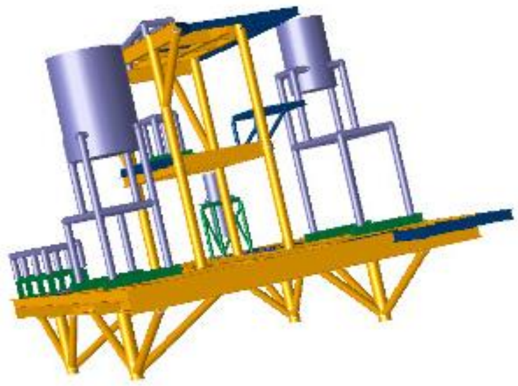

Fig. 7: Geometric design of modules in SACS software

3.2. 2. Second Model

This model has four supports equipped with neoprene. All assumptions of acceleration, wind speed, weight, etc. are similar to the ones discussed above. The geometric design of this model is the same as the first model according to Figure 7.

3.2.3. Studied Members

The studied module is divided into two parts according to Figure 8. The first part consists of members that are directly connected to the stools, and the second part is comprised of members of the main deck and other members of the upper level. These members are shown in Figures 9 and 10. In both models, the mentioned members are examined, and the results of modelling are presented.

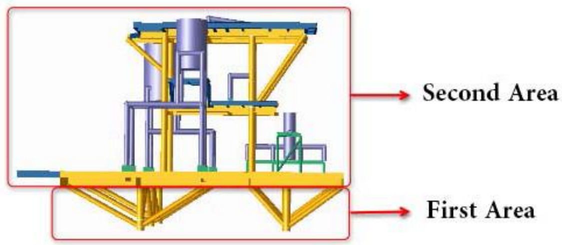

Fig. 8: Areas studied module

Fig. 9: Studied Members of First Area

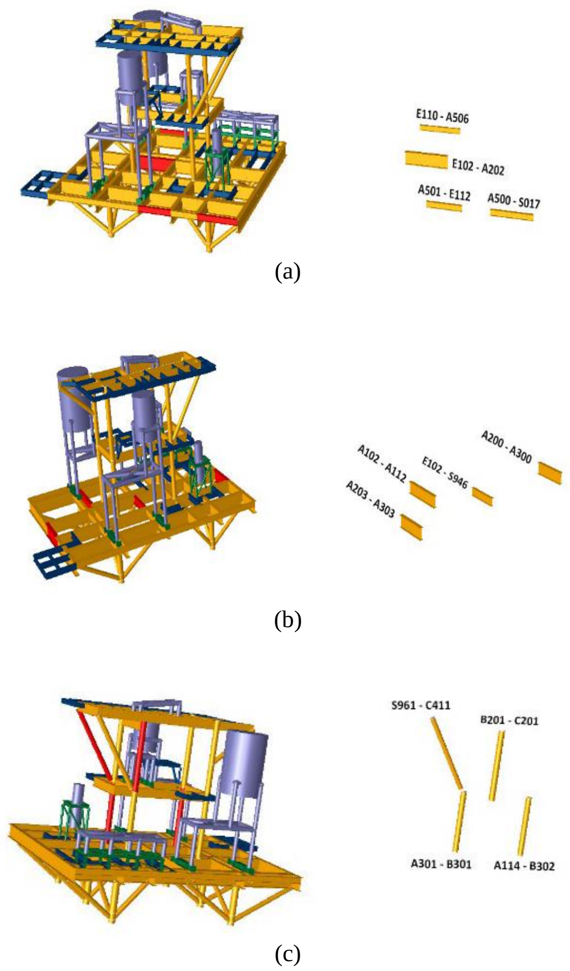

Fig. 10: Studied members of the second area in the X, Y and Z directions

4. Modeling Results

The results of the simulations are presented by comparing the UC Ratio between the studied members in the first and second models. Note that the models are just different in module supports. According to the classification given in Fig. 8, in the first region, the members of each group have the same sections, but for the studied members of the second region shown in Figures 10 (a) and (b), it is necessary to pay attention to the variations in different sections. The members of the STX group in the first model are directly installed on the stools, but in the second model, they are placed on the neoprenes. The members of the ST1 group are in the Z-axis direction and connect the main deck to the members of the STX group. The ST2 group comprises of diagonal members that are connected to the STX members from one side to the bottom of the main module and to the members of the STX group. As shown in Figure 9, these members are placed in different rows of the module. The comparisons have been presented as graphs with member's UC ratio criteria.

In the STX group of the second model, the average UC ratio reduction of 76% was recorded in comparison with the first model. Members that are directly on Neoprene are seen to have a higher reduction stress in comparison with their upper members. Note that members of the ST1 group stand on STX members according to Figure 10. Members S021-A102 and S023-A402, according to the results presented in Fig. 11 (b), tolerate less UC ratio in comparison with the other two members of the group due to being placed in a part of the module with less equipment on it. It should be noted that the four members of the STX group, which in Figure 11 (a) have a lower UC ratio than other members, are among the two members listed in the ST1 group. According to Fig.11(b) , in ST1 group members, the second model has a significant reduction of 64.84% UC ratio relative to the first model. By examining the members of the first region, it is clear that in all members of this region in the second model, we face a significant reduction in UC ratio. In the ST2 group, in the second model, the average reduction of 55.56% was recorded as relative stress.

The behaviour of the members of the second region differs from that of the first one. In these members, there is either no change in their relative tensions or they have been increased. According to Fig. 12 (a), there has not been a significant change in the studied members in the longitudinal direction of the ship. In the studied members, along with the transverse ship, the average UC ratio was 0.33, which was accompanied by an increase of 32.87%. According to Fig. 11 (c), the relative stress variation along the vertical axis is not significant.

The results are divided into three categories: the first group of members which were reduced, the second group of members which were unchanged, and the third group which was accompanied by an increase in relative stress compared to the first model.

The first category comprises of all the supporting members of the first region. These members are deployed according to figure 8 under the main deck and precisely on neoprene. These members have been associated with a significant reduction in relative stress. This amount of UC ratio ranges from 25 to 85 percent. In the first region, the relative reduction of 60% was recorded.

The second category includes the studied members of the longitudinal and vertical directions of the ship. According to Figures 12 (a) and (c), no significant change was observed in these members.

The third category of the studied members is the transverse direction of the ship. To analyse the performance of these members, the explanations given in Table 6 are referenced.

According to the position of the studied module, those located in low distance with longitudinal direction and far distance transverse direction, have a critical roll and low pitch motion. In equations 2, 3 and 4, the acceleration in the Y direction receives the largest impact of the roll motion.

According to linear acceleration from Table (1), the acceleration in the Y and Z direction is greater than the X direction. So, according to equations 3 and 4, rolling motion of ship has the greatest effect on the linear acceleration in the direction Y and Z.

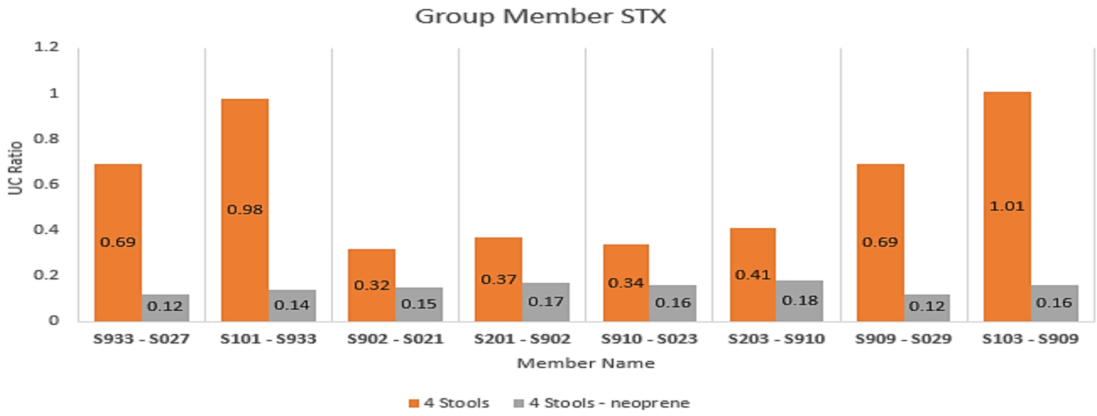

(a)

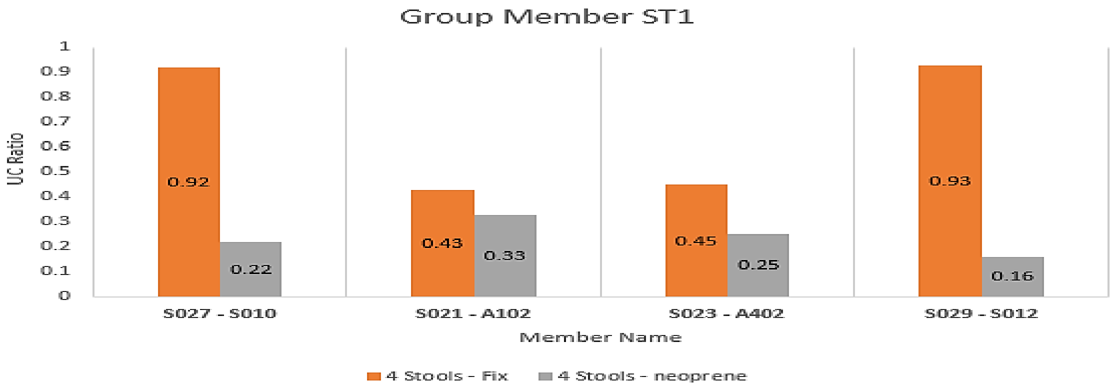

(b)

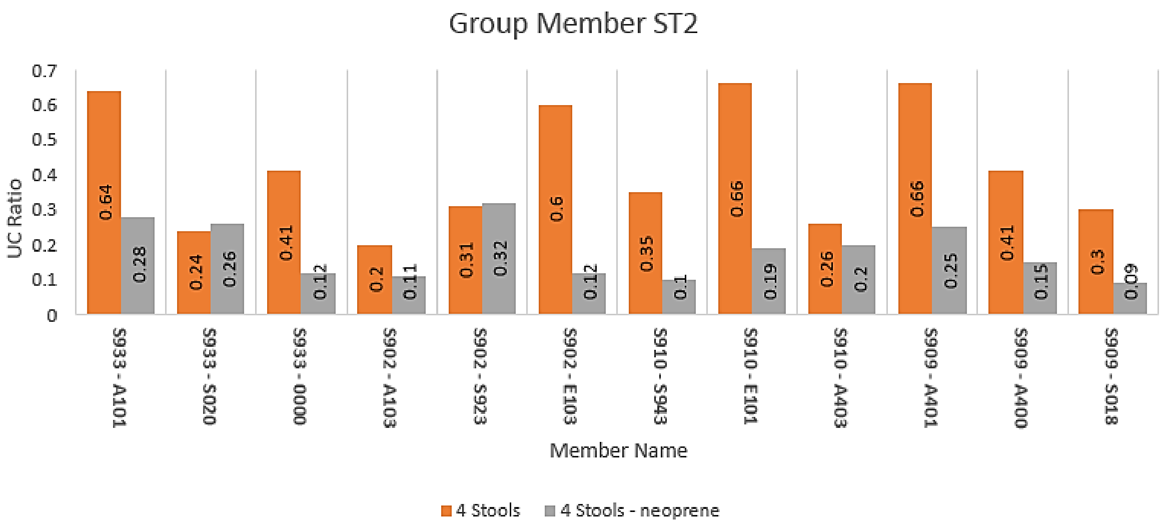

(c)

Fig. 11: Diagram of the Comparison between the members of the first area in the first a second model (a) STX group (b) ST1 group (c) ST2 group

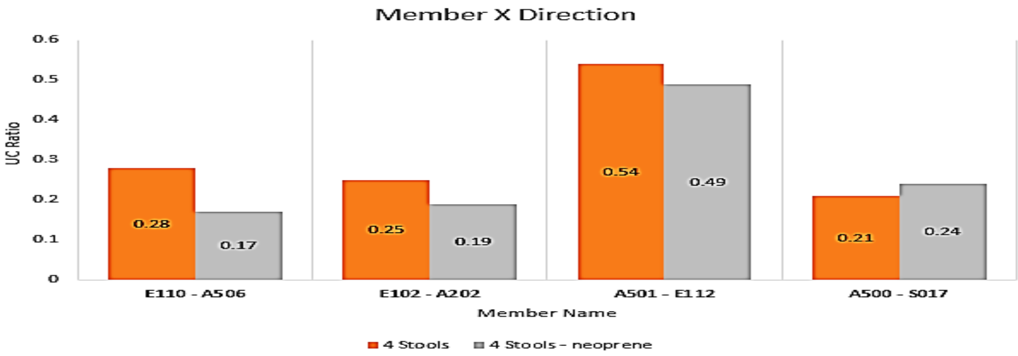

(a)

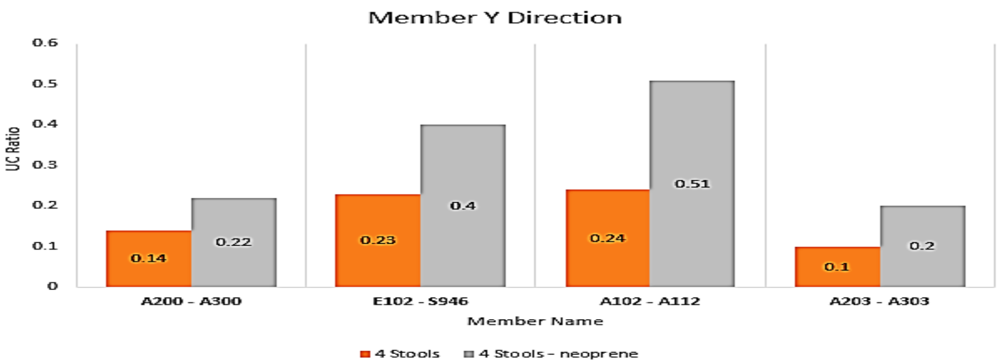

(b)

(c)

Fig. 12: Diagram of the Comparison between the members of the second area in the first a second model (a) X direction (b) Y direction (c) Z direction

Ax is the total positive acceleration along X axis in m/s:

$$A_X = \pm\gamma_{Su} - g.\sin(\pm\theta_P) \qquad (2)$$

AY is the total positive acceleration along Y axis in m/s

$$A_Y = \pm\gamma_{Sw} + g.\sin(\pm\theta_r) \qquad (3)$$

Az is the total positive acceleration along Z axis in m/s

$$A_Z = \pm\gamma_H + g.(\cos(\pm\theta_r)\ .\ \cos(\pm\theta_P) - 1) \qquad (4)$$

Extreme angular displacement has caused the inertia load to have the greatest effect on the design of the module existing as a critical factor. So, the increasing acceleration in each direction, should see an increase in the UC ratio in it. This means that if the acceleration increases, UC ratio will also increase in that direction. For this judgment, the second model is redesigned with the Ballast acceleration condition shown in Table 6. Then the results of the analysis will be presented. As expected, with an increasing Roll motion in ballast condition, AY and AZ exhibit a further increase in the acceleration. Therefore, the second model is analyzed with the acceleration of the ballast condition and the increase in relative stress of 10% to 30% in the Y direction studied members. These results are presented in Table 12 and Figure 13.

Table 6. Acceleration Values for Ballast Condition

Condition	*Acceleration Value (g)*		
	Ax	*Ay*	*Az*
1 Year	0.068	0.091	0.171
10 Years	0.081	0.176	0.200
50 years	0.084	0.213	0.209

Table 7. The UC ratio of the studied members for Y direction in Ballast and Full Load condition

	Full Load Condition		Ballast Condition	
Member	1 /A200 - A300		2 /A200 - A300	
Module	UC Ratio	Percentage change	UC Ratio	Percentage change
4 Stools	0.14	-	0.14	-
4 Stools - neoprene	0.22	+57.14	0.26	+85.71
Member	3 /E102 - S946		4 /E102 - S946	
Module	UC Ratio	Percentage change	UC Ratio	Percentage change
4 Stools	0.23	-	0.25	-
4 Stools - neoprene	0.4	+73.91	0.46	+84.00
Member	5 /A102 - A112		6 /A102 - A112	
Module	UC Ratio	Percentage change	UC Ratio	Percentage change
4 Stools	0.24	-	0.24	-
4 Stools - neoprene	0.51	+112.50	0.54	+125.00
Member	7 /A203 - A303		8 /A203 - A303	
Module	UC Ratio	Percentage change	UC Ratio	Percentage change
4 Stools	0.1	-	0.1	-
4 Stools - neoprene	0.2	+100.00	0.23	+130.00

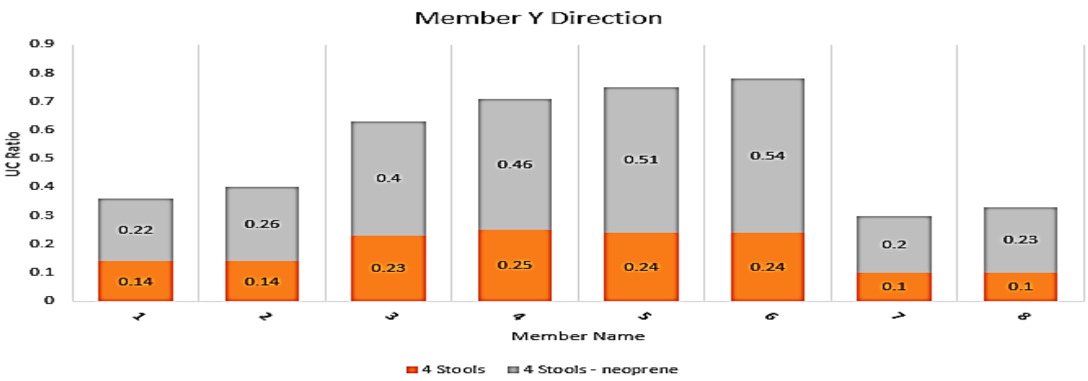

Fig. 13: Compare the studied members for Y direction in Ballast and Full Load condition

5. Conclusion

In the first step, the whole module was divided into two general areas. In the first area, all the members were associated with a decrease in relative stress by more than 50%. But members of the second area reacted to the change in support in two ways. The X and Z direction members remained unchanged to relative stress, but in the Y direction members, the presence of neoprene had a negative effect and increased the relative stress.

The study showed that this module has a critical roll angular acceleration due to its position on the ship deck, which has the highest effect in linear acceleration in the Y direction according to Formula 1.

Generally, base isolation causes reduction in base reaction of installed modules. If install modules are sensitive to displacement, more caution shall be applied in base isolation selection. With regard to the diverse responses of deck under wave hitting in different locations, base isolation stiffness is an important parameter to be considered in structural design and response.

As a general conclusion, it should be noted that the effect of neoprene depends on the amount and direction of acceleration. Since the deck of the ship is very large and the acceleration values are varied in different parts of the deck, the neoprene for each module must be examined according to the position of the module on the deck and its acceleration values.

References:

[1] Lapidaire, P. J. M., and P. J. Leeuw. "The effect of ship motions on FPSO topsides design." In Offshore Technology Conference. Offshore Technology Conference, 1996.

[2] Ørbeck-Nilssen, Knut, and Tom Haug. "New Standards and Services for Design of Offshore Structures." In Offshore Technology Conference. Offshore Technology Conference, 2000.

[3] Wolford, Andrew J., James C. Lin, James K. Liming, Andrew Lidstone, and Robert E. Sheppard. "Integrated risk based design of FPSO topsides, structural and marine systems." In Offshore Technology Conference. Offshore Technology Conference, 2001.

[4] François, Michel, and Ulrik Frorup. "Design Criteria and Inspection Strategy for FPSO's." In Offshore Technology Conference. Offshore Technology Conference, 2002.

[5] Han, Hans, Jung Han Lee, and Yong Soo Kim. "Design development of FSRU from LNG carrier and FPSO construction experiences." In Offshore Technology Conference. Offshore Technology Conference, 2002.

[6] Krekel, M. H., and M. L. Kaminski. "FPSOs: Design Considerations for the Structural Interface Hull and Topsides." In Offshore Technology Conference. Offshore Technology Conference, 2002.

[7] Thomas, P. A., et al. "A solution for FPSO module integration." Offshore Technology Conference. Offshore Technology Conference, 2003.

[8] Wang, Ge, and Robert Spong. "Experience based data for FPSO's structural design." In Offshore Technology Conference. Offshore Technology Conference, 2003.

[9] Thomas, P. A., S. Malek, N. Tcherniguin, and V. Bestel. "A solution for FPSO module integration." In Offshore Technology Conference. Offshore Technology Conference, 2003.

[10] Huijsmans, R. H. M., and J. P. Borleteau. "The Flow Around FPSO's in Steep Regular Waves." In The Thirteenth International Offshore and Polar Engineering Conference. International Society of Offshore and Polar Engineers, 2003.

[11] Chakrabarti, Subrata. Handbook of offshore engineering, pp. 419-661. 2005.

[12] Buchner, Bas, and Tim Bunnik. "Extreme wave effects on deepwater floating structures." In Offshore Technology Conference. Offshore Technology Conference, 2007.

[13] Molland, Anthony F. "A guide to ship design, construction and operation." The Maritime Engineering Reference Book (2008): 636-638.

[14] M, Lars O Henriksen, Boyden D Williams M, Xiaozhi Wang M, and Donald Liu F. 2008. "Structural Design and Analysis of FPSO Topside Module Supports, " no. October: 155–64.

[15] Metzger, Bernhard H., Donald A. Salmond, and Alan Tilstone. "FPSO Environmental-Risk Management." SPE Economics & Management 2, no. 01 (2010): 38-50.

[16] Chen, Jay, Chris Hartman, Bryan Margo, and Tony Owen. "Topsides Facilities Design and Module-to-Vessel Interface." In Offshore Technology Conference. Offshore Technology Conference, 2011.

[17] Mespaque, Wagner, Vitor José Frainer, and Paulo Roberto de Freitas Teixeira. "Analysis of hull–topside interaction by experimental approach on floating production unit P-53." Applied Ocean Research 37 (2012): 133-144.

[18] Hirdaris, S. E., W. Bai, Daniele Dessi, Ayşen Ergin, X. Gu, O. A. Hermundstad, R. Huijsmans et al. "Loads for use in the design of ships and offshore structures." Ocean engineering 78 (2014): 131-174.

[19] Su, Zhiyong, Yong Luo, Xiaoliang Qi, and Yi Xie. "FPSOS for Deepwater Applications." In Offshore Technology Conference-Asia. Offshore Technology Conference, 2014.

[20] Zanganeh, Razieh, and Krish Thiagarajan. "Prediction of the mean heading of a turret moored FPSO in bi-modal and bi-directional sea states." Applied Ocean Research 78 (2018): 156-166.

[21] Sanchez-Mondragon, J., et al. "Yaw motion analysis of a FPSO turret mooring system under wave drift forces." Applied Ocean Research 74 (2018): 170-187.

[23] Veritas, Det Norske. "Recommended Practice DNV-RP-C101–Allowable Thickness Diminution for Hull Structure of Offshore Ships." Hovik, Norway (2007).

[24] Det Norske Veritas. "DNV-OS-C102 Structural Design of Offshore Ships, " no. October. 2012.

[25] For, Guide. " ABS - Dynamic Loading Approach ’ for Floating Production , Storage and Offloading (FPSO) Installations." Analysis.2010.

[26] API, RP. (2000). 2A-WSD. Recommended practice for planning, designing and constructing fixed offshore platforms-working stress design, 21

[27] Dezvareh, Reza. "Evaluation of turbulence on the dynamics of monopile offshore wind turbine under the wave and wind excitations." Journal of Applied and Computational Mechanics5, no. 4 (2019): 704-716.